Effect of Particle Size and Shape on the Infrared Absorption of Magnesium Oxide Powders*

JAMES T. LUXON,† DONALD J. MONTGOMERY, AND ROBERT SUMMITT
Department of Metallurgy, Mechanics and Materials Science, Michigan State University, East Lansing, Michigan 48823

(Received 22 July 1969)

Magnesium oxide powders obtained from three sources exhibit strikingly different infrared absorption spectra. These differences are correlated herein with variations in the size and shape of the particles in the powders, and are interpreted in terms of both Fröhlich-type (surface) modes and classical electromagnetic scattering theory. (1) Reagent-grade MgO powder exhibits a strong and broad absorption centered at 550 cm^{-1}, the position of which is determined by the Fröhlich-type fundamental frequency for spherical particles that are small compared with the radiation wavelength. The absorption broadening results from variations in particle size and shape. The presence of double particles gives rise to a secondary absorption near 460 cm^{-1}. (2) MgO smoke in various matrices absorbs strongly at the bulk-mode frequency (401 cm^{-1}) owing to the presence of both individual large cubical particles and long chains of small cubical particles. A second strong absorption occurs at 490 cm^{-1} in Nujol, or at 546 cm^{-1} on polyethylene plates; these frequencies represent a surface mode of small MgO cubes. A shoulder at still higher frequencies is ascribed to surface modes of rod-shaped particles. (3) MgO powder obtained from thermally decomposed $MgCO_3$ absorbs strongly at the bulk-mode frequency (401 cm^{-1}), because of the presence of large flakelike particles having a very fine grain structure. With increasing grain size, the principal absorption shifts to lower frequencies, and a secondary absorption, near 490 cm^{-1} in Nujol, appears as a result of absorption by small MgO particles.

THE optical properties of bulk ionic crystals in the region of a fundamental lattice absorption are well understood in terms of the interaction of photons with long-wavelength polar phonons. In the theory of this interaction, the specimen dimensions are commonly assumed to be infinite in directions perpendicular to the direction of radiation propagation for the case of transmission through, or reflection from, thin films. For reflection from bulk crystals, all dimensions are assumed to be infinite.

Very little attention has been given to the case where more than one dimension of the specimen is comparable with the radiation wavelength. Indeed, infrared absorption spectra of powdered materials often are reported without any consideration of the effect that size and shape of the particles may have on the spectra. A few studies, however, have indicated the potential usefulness of the existing theoretical tools. Hass[1] has prepared NaF and LiF specimens in the form of elliptical cylinders of semi-infinite length by evaporating the materials onto gratings. Through an extension of Fröhlich's results[2] he satisfactorily interpreted as a size effect the infrared absorption at different frequencies of radiation polarized parallel and perpendicular to the grating lines. Summitt[3] applied with success a similar interpretation to the infrared absorption spectrum of fibrous β-SiC. Powders of materials having a more complex crystal structure, viz., SnO_2 and TiO_2 (rutile), have been treated by Summitt[4] and by Luxon and Summitt[5] through both a generalization of Fröhlich's results and classical electromagnetic scattering theory.

To corroborate and extend these approaches to interpreting the spectra of powdered materials, we have investigated MgO, which can be prepared as particles of rather well-defined and controlled size and shape. MgO has the further advantage of having been throughly studied in the form of single crystals, both optically[6] and by inelastic neutron scattering.[7] The results of the optical and neutron scattering studies are in good agreement, indicating the fundamental-mode transverse-optical-mode (TO) frequency to be $\sim$401 cm^{-1}. In the present work we show that by taking account of the size and shape of the powder particles, the main features of the absorption spectra of three different forms of MgO powder can be reconciled with the results from large single crystals.

I. THEORY

The infrared absorption spectrum of a polar crystalline powder may be analyzed according to either of two schemes.[5]

A. Scheme 1

A spherical specimen of an isotropic polar crystal will absorb radiation at the frequency ν_s different from the TO frequency of the bulk crystal, ν_t, when the

* Based upon a thesis submitted by J. T. Luxon in partial fulfillment of the requirements for the Ph.D. degree at Michigan State University.

† National Science Foundation Faculty Fellow. Present address: General Motors Institute, Flint, Mich.

[1] M. Hass, Phys. Rev. Letters **13**, 429 (1964).

[2] H. Fröhlich, *Theory of Dielectrics* (Clarendon Press, Oxford, 1958).

[3] R. Summitt, Spectrochim. Acta **23**, 2857 (1967).

[4] R. Summitt, J. Appl. Phys. **39**, 3762 (1968).

[5] J. T. Luxon and R. Summitt, J. Chem. Phys. **50**, 1366 (1969).

[6] J. R. Jasperse, A. Kahan, J. N. Plendl, and S. S. Mitra, Phys. Rev. **146**, 526 (1966).

[7] K. H. Reider and E. M. Hörl, Phys. Rev. Letters **20**, 209 (1968).

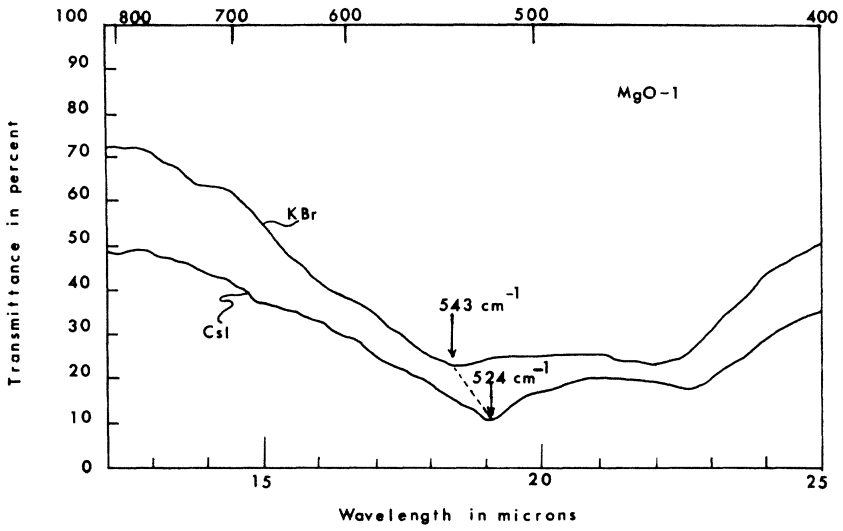

FIG. 1. Infrared absorption of commercial MgO powder (MgO-1) in KBr and CsI pellets: D. J. Montgomery and K. F. Yeung (unpublished).

specimen diameter is small compared with the phonon wavelength of the TO mode. The two frequencies are related by

$$\nu_s/\nu_t=[(\epsilon_0+2\epsilon_m)/(\epsilon_\infty+2\epsilon_m)]^{1/2}, \quad (1)$$

where ϵ_0 and ϵ_∞ are the static and high-frequency dielectric constants of the crystal, respectively, and ϵ_m is the dielectric constant of the medium surrounding the specimen.

This result has been generalized[8] for the case (a) where the crystal lattice is of symmetry lower than cubic and hence has more than one TO frequency, (b) where the oscillations are damped, and (c) where the particles are ellipsoidal. In case (c), for a crystal having but a single triply degenerate infrared-active lattice mode, the result is

$$\nu_s/\nu_t=[(\epsilon_0-1)g+\epsilon_m]/[(\epsilon_\infty-1)g+\epsilon_m]. \quad (2)$$

An equation of this form is to be applied to each of the principal axes of the ellipsoid, where g is a shape factor with a value between zero and unity, and ν_s and ν_t are the oscillator frequencies in the absence of damping. The difference between the undamped and damped frequencies is negligible except in extreme cases, and for MgO the distinction may be neglected.

B. Scheme 2

The extinction cross section C^{ext} for the loss of energy from a beam of electromagnetic radiation incident on ellipsoidal particles smaller than the radiation wavelength and of arbitrary eccentricity consists of a sum of a pure scattering cross section C^{sca} and a pure absorption cross section C^{abs}:

$$C^{\text{ext}}=C^{\text{abs}}+C^{\text{sca}}. \quad (3)$$

These cross sections are given approximately by

$$C^{\text{abs}}=-4\pi(2\pi/\lambda)\,\text{Im}(\alpha) \quad (4)$$

and

$$C^{\text{sca}}=(8\pi/3)(2\pi/\lambda)^4|\alpha|^2, \quad (5)$$

where λ is the radiation wavelength and α is the polarizability for a particular principal axis of the ellipsoid. The polarizability is related to particle volume V, polarization (shape) factor g, and the complex refractive index $m=n-ik$ by the equation

$$V/4\pi\alpha=g+1/(m^2-1). \quad (6)$$

The shape factor g has the value $\frac{1}{3}$ for the case of a sphere. When absorption is present, C^{abs} is the dominant term unless the specimen dimensions are comparable with the radiation wavelength.

Although contributions to the absorption by surface modes already are included in the calculation of C^{ext}, as shown by Ruppin and Englman,[9] it is useful, nevertheless, to examine explicitly the limiting frequencies at which surface modes may contribute to absorption. For spheres with dielectric constant ϵ (see Ref. 9), the electric-type modes (or *surface* modes, arising from long-range forces) occur at frequencies given by

$$\epsilon\{k^0Rn_l(k^0R)\}'j_l(k^iR)=\{k^iRj_l(k^iR)\}'n_l(k^0R), \quad (7)$$

and the magnetic-type modes (or *bulk* modes, due to short-range forces) at frequencies given by

$$j_l(k^iR)\{k^0Rn_l(k^0R)\}'=n_l(k^0R)\{k^iRj_l(k^iR)\}'. \quad (8)$$

In Eqs. (7) and (8), j_l and n_l are, respectively, Bessel and Neumann functions, k^i is $\epsilon^{1/2}2\pi\nu/c$, k^0 is $2\pi\nu/c$, and R is the particle radius. Differentiation with respect to the argument of the Bessel or Neumann function is indicated by a prime. For $kR\ll1$, $n_l\cong(kR)^{-(l+1)}$, and

[8] J. T. Luxon, Ph.D. thesis, Michigan State University, 1969 (unpublished).

[9] R. Ruppin and R. Englman, J. Phys. C1, 630 (1968).

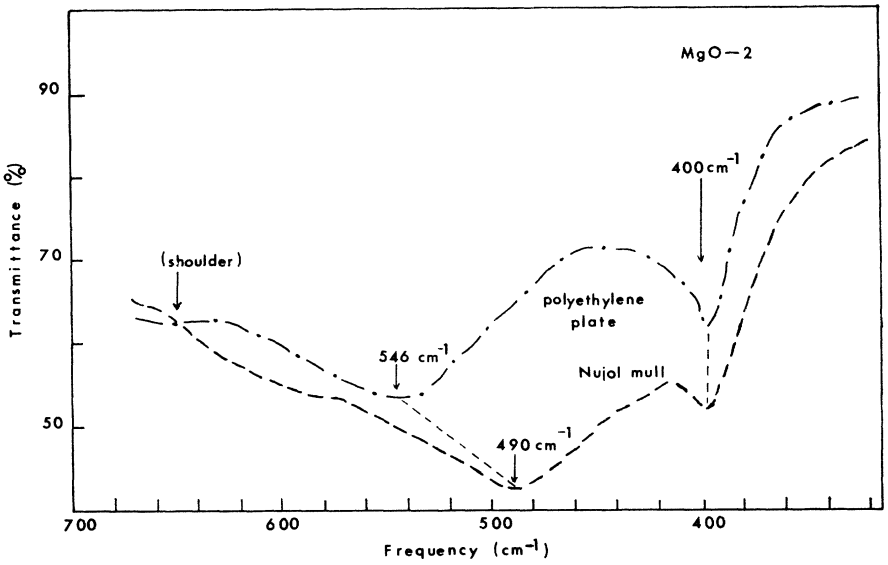

FIG. 2. Infrared absorption of MgO smoke (MgO-2) deposited on polyethylene plates and dispersed in Nujol.

$j_l \cong (kR)^l$ when

$$\epsilon = -(l+1)/l, \quad l = 1, 2, 3, \cdots \tag{9}$$

for the electric modes. Equation (8) need not be considered further, since in the present approximation the number of magnetic modes, which is proportional to the volume, approaches zero. With a dielectric constant of the form

$$\epsilon = \epsilon_\infty + (\epsilon_0 - \epsilon_\infty)/(1 - \nu^2/\nu_t^2), \tag{10}$$

Eq. (9) gives

$$(\nu_s/\nu_t)^2 = [\epsilon_0 + (l+1)\epsilon_m/l]/[\epsilon_\infty + (l+1)\epsilon_m/l], \tag{11}$$

where ϵ_m has been included to account for the refractive index of the surrounding medium. Equation (11) reduces to Fröhlich's relation, Eq. (1), for $l=1$. For $l=\infty$, it gives the maximum surface-mode frequency. The total number of modes is not infinite; rather, it is proportional to the surface area.

II. EXPERIMENTAL PROCEDURE

Magnesium oxide was studied in three different forms.

(1) MgO powder obtained commercially from various sources and of varying impurity content. All specimens were at least 99% pure, and no features of the spectra

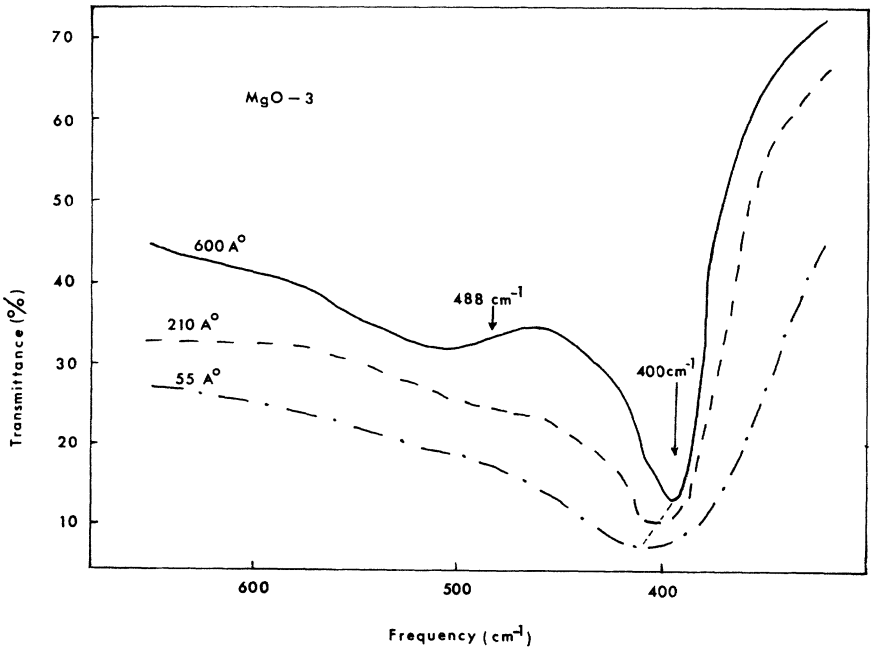

FIG. 3. Infrared absorption of MgO from thermal decomposition of $MgCO_3$ (MgO-3) of varying grain sizes.

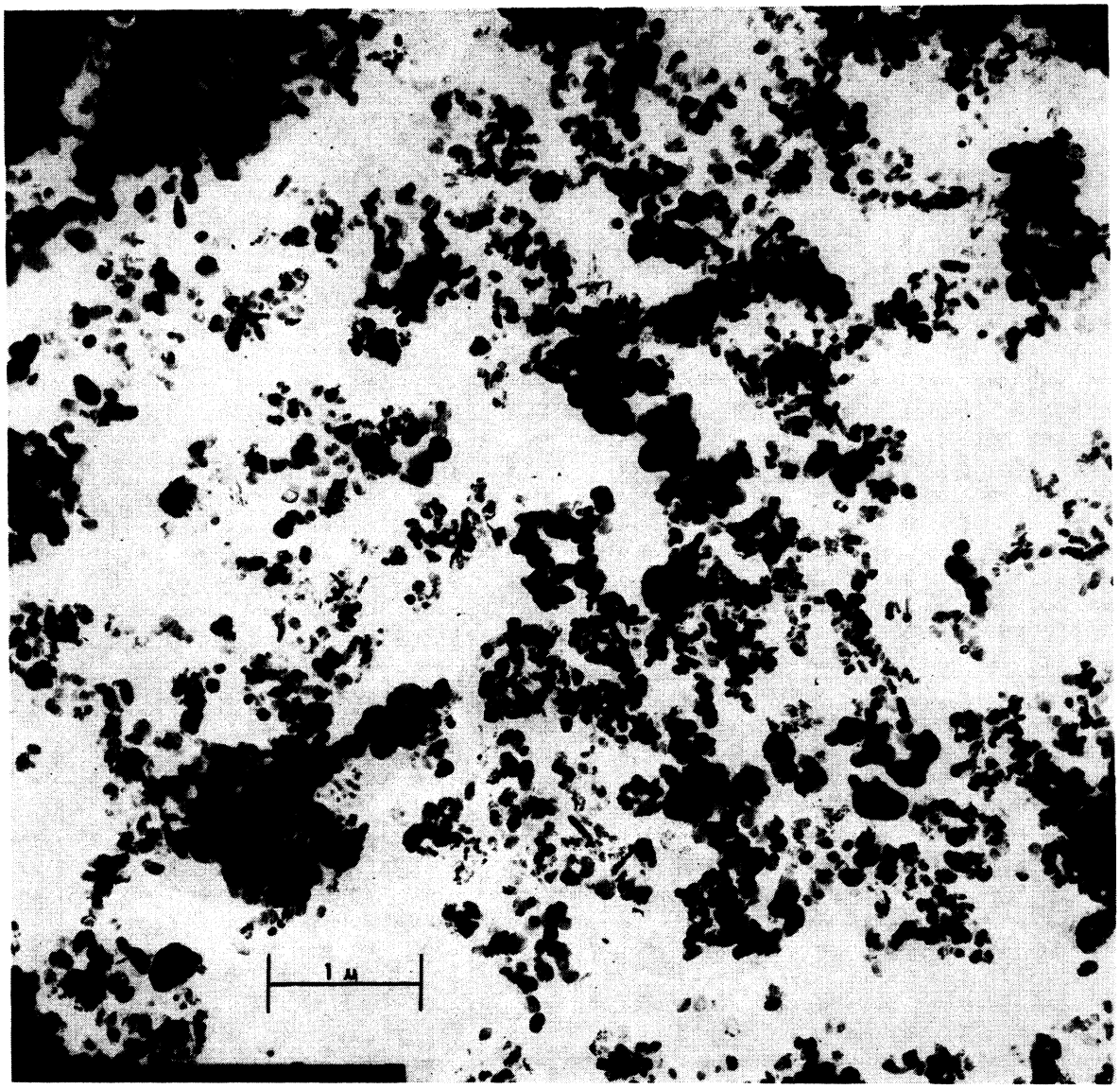

FIG. 4. Electron micrograph of commercial-grade MgO powder (MgO-1). Magnification 23 400×.

could be attributed to impurities. This material will be called MgO-1.

(2) MgO powder as smoke, formed by burning 99.7%-pure Mg ribbon in air or oxygen, and depositing the resulting MgO on polyethylene or alkali-halide plates. This material will be called MgO-2.

(3) MgO powder obtained by thermal decomposition of $MgCO_3$ in air. Long sintering times at a given temperature result in large grains of quite uniform size distribution. Higher temperatures at fixed times also stimulate the growth of larger grains. By control of these factors, powders with particles of practically any average grain size from 50 to 100 Å or even larger can be obtained.[10] Grain sizes, as determined by electron microscopy, agreed well with the literature values for given annealing times and temperatures. This material will be called MgO-3.

The spectra of MgO-1 powders (Fig. 1) were obtained with a Perkin-Elmer Infracord KBr spectrophotometer with range 12.5–25 μ (800–400 cm^{-1}), the specimen being dispersed in alkali-halide powder and pressed into pellets. The spectra of MgO-2 powder (Fig. 2) were recorded with a Perkin-Elmer model 301 spectrophotometer operated in the range 667–300 cm^{-1}. Spectra were obtained for (a) MgO smoke deposited directly onto polyethylene plates and (b) smoke carefully scraped from a polyethylene plate into Nujol and dispersed by means of a Wig-L-Bug vibrator. The spectra of

[10] L. S. Birks and H. Friedman, J. Appl. Phys. 17, 687 (1946).

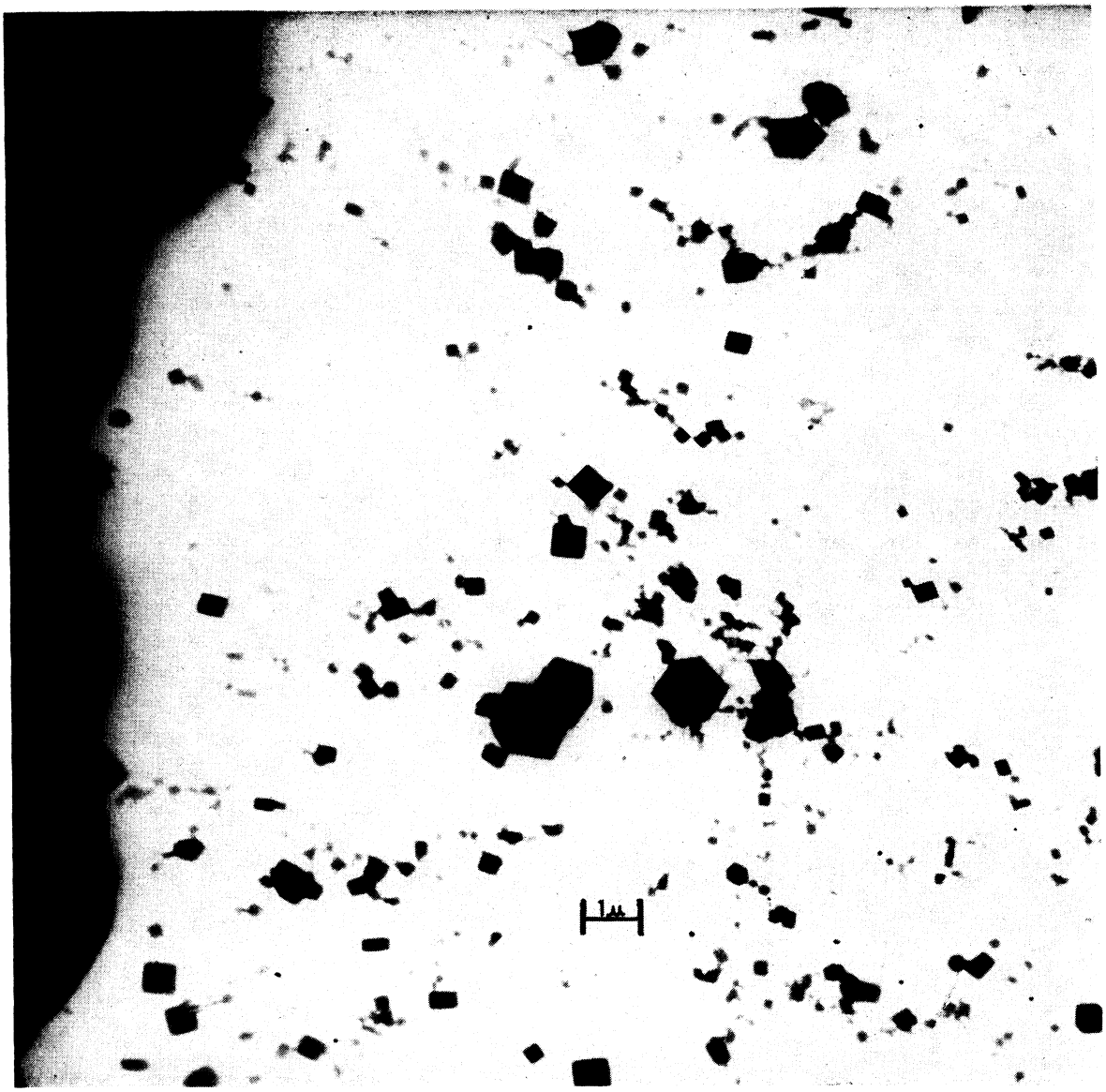

FIG. 5. Electron micrograph of MgO smoke (MgO-2) obtained by burning Mg ribbon in air. Magnification 7000×.

MgO-3 powder (Fig. 3) were obtained in the 667–170-cm^{-1} range with the model 301 spectrophotometer, and were extended to 800 cm^{-1} with the Infracord. The powders were dispersed in Nujol and the resulting mull was placed between polyethylene or KBr plates. Variations in length of time for dry grinding and Nujol grinding on the Wig-L-Bug vibrator produced no noticeable differences in the spectra.

III. RESULTS

A. Absorption Spectra

Spectra of the three types of MgO powder are quite different, as seen in Figs. 1–3. For all three forms, however, the main absorption is contained from about 385 to about 740 cm^{-1}. MgO-2 and MgO-3 both show strong absorption at about 400 cm^{-1}, and MgO-3 begins to show a distinct absorption band at around 490 cm^{-1} as the grain size increases. The maximum absorption of MgO-2 occurs at 546 cm^{-1} for smoke deposited on polyethylene, shifting to 490 cm^{-1} for the smoke dispersed in Nujol. The higher-frequency absorption maximum of MgO-1 varies with the refractive index of the matrix medium, moving from 543 cm^{-1} for KBr to 524 cm^{-1} for CsI (Fig. 1). MgO-1 and MgO-2 also reveal secondary absorptions which shift with refractive index of the medium.

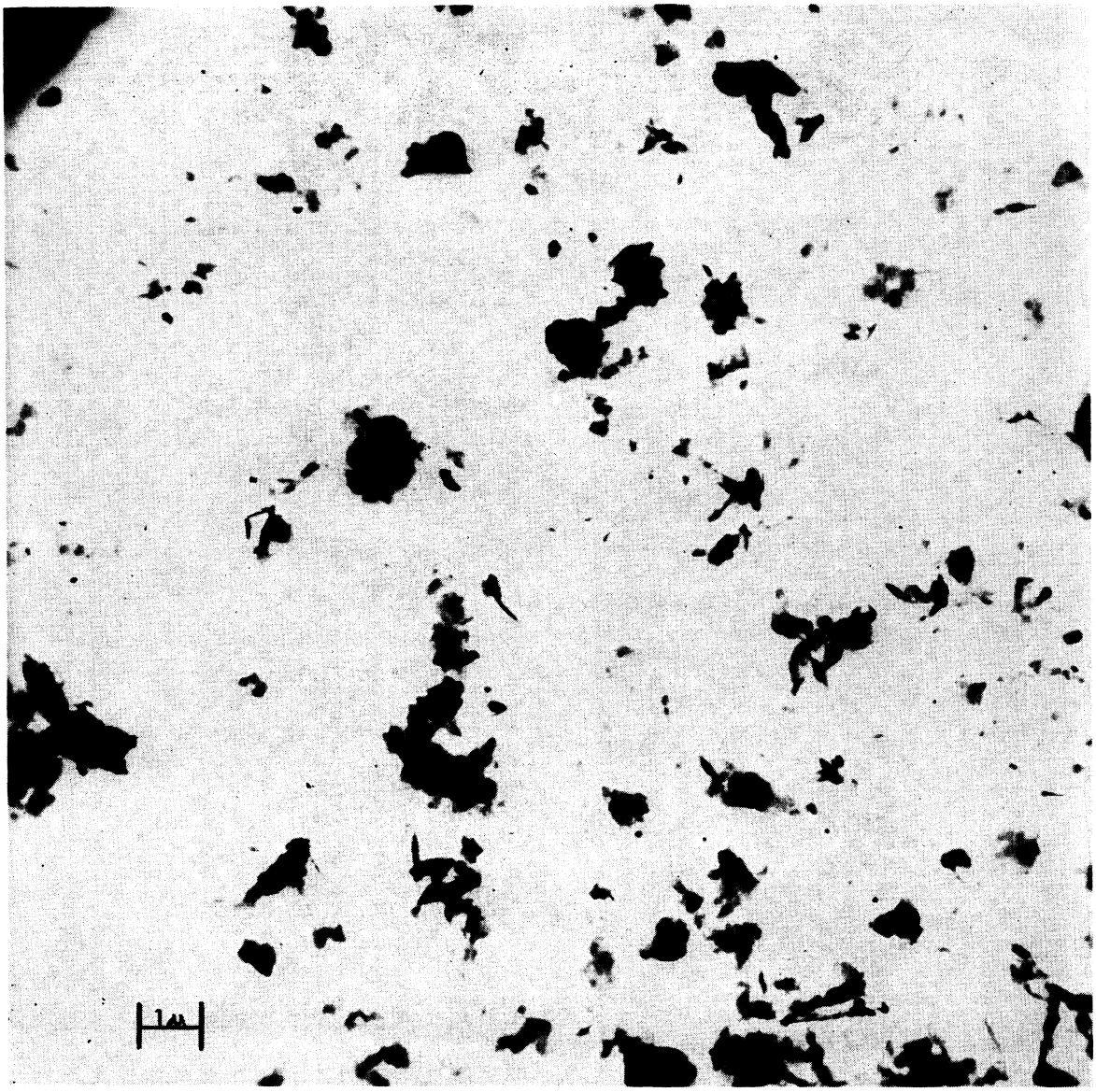

FIG. 6. Electron micrograph of MgO obtained by thermal decomposition of $MgCO_3$ (MgO-3), 60 Å grain size. Magnification 7000×.

B. Microscopic Classification

(1) Commercial MgO-1 powder, when fresh from the bottle, contains particles several microns in diameter as verified by optical microscopy. These larger particles, upon dry grinding in the Wig-L-Bug, break up into smaller ones of $\frac{1}{2}$ μ or less on a side, and irregular shape, the final powder containing a negligible amount of larger particles, as may be seen in Fig. 4. Wet grinding in Nujol produces essentially the same result.

(2) MgO-2 smoke particles are nearly perfect cubes, frequently stacked in staggered fashion to form chain-like aggregates. Figure 5 is an electron micrograph of MgO-2 collected directly on a Formvar-coated copper grid. MgO-2 deposited from water suspension followed by evaporation has essentially the same appearance. Many of the single cubes are 1.5 μ or more on an edge, whereas the chains mostly are composed of smaller cubes, 0.3 μ or less, stacked in chains as long as 1.5 μ.

(3) MgO-3 powders are in the form shown in the electron micrographs of Figs. 6–8. The measured grain sizes agree well with the values given by Nicholsen[11] for corresponding annealing times and temperatures. The particles are somewhat plateletlike, several microns across, and composed of very fine grains (Fig. 6).

[11] M. M. Nicholsen, Proc. Roy. Soc. (London) **A228**, 490 (1955).

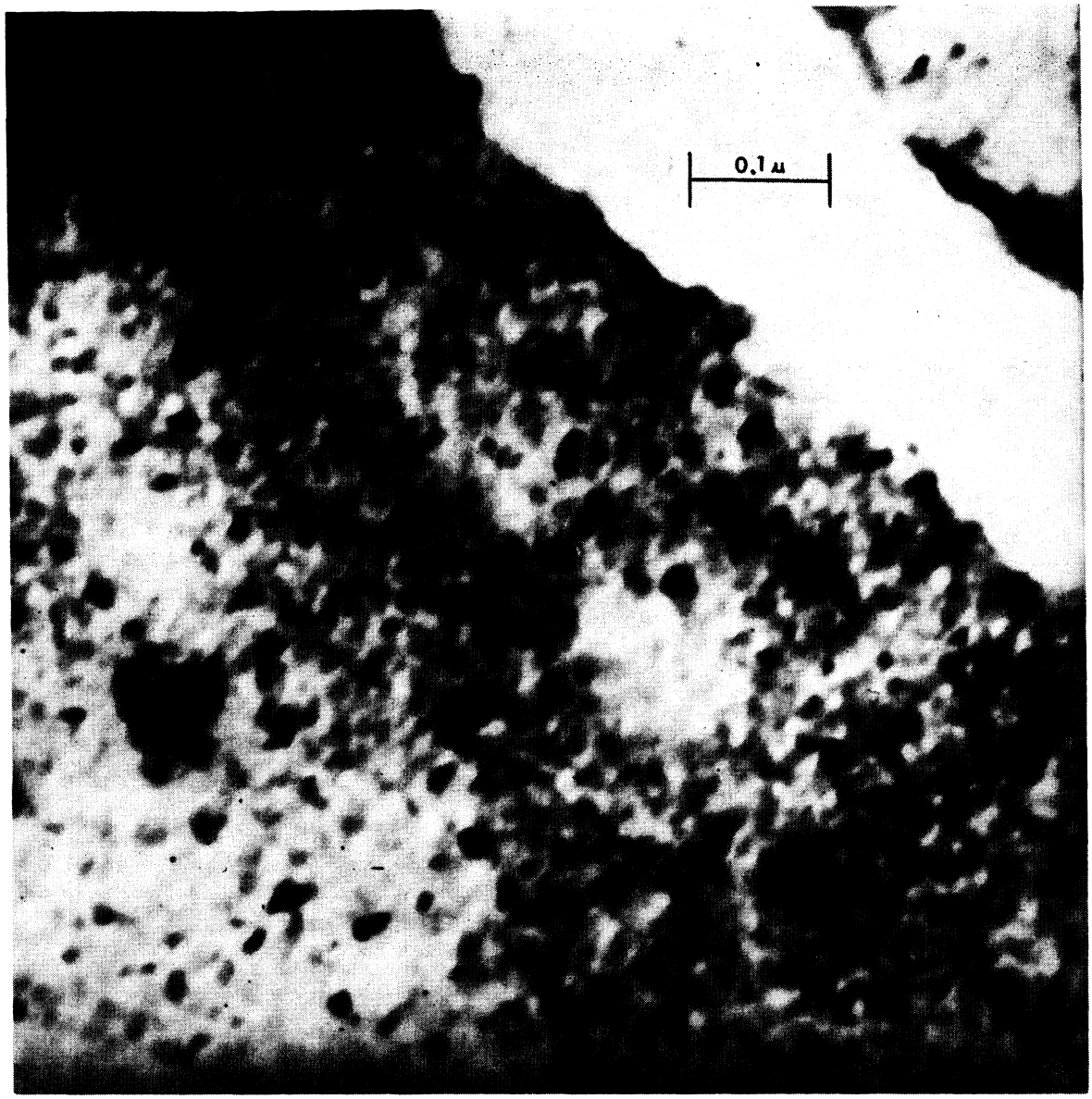

FIG. 7. Electron micrograph of MgO obtained by thermal decomposition of $MgCO_3$ (MgO-3), 100 Å grain size. Magnification 200 000×.

IV. INTERPRETATION

For small MgO spheres imbedded in a matrix of refractive index 1.5, the extinction cross section as calculated by Eq. (3) has its maximum at 550 cm^{-1}. Computation of the complex refractive index of MgO in this calculation was based on parameters (Table I) given by Jasperse *et al.*,[6] who used a two-oscillator model to fit the reflectivity data of single-crystal MgO.

The low-strength 640-cm^{-1} oscillator contributes very little to the calculated extinction cross section, and has no effect on the position of the absorption maximum. The Fröhlich relation, Eq. (1), also yields 550 cm^{-1} for the expected position of the absorption maximum for spheres in a matrix of refractive index 1.5. Both experimental maximum-absorption frequency and calculated maximum-absorption frequency [Eq.

TABLE I. MgO optical parameters based on the single-crystal-reflection dispersion analysis of Jasperse *et al.* (Ref. 6).

Mode	Frequency ν_t (cm^{-1})	Strength $4\pi\rho$	Damping γ (cm^{-1})
1	401	6.60	0.019
2	640	0.45	0.160
	Dielectric constants		
	$\epsilon_\infty = 3.01$	$\epsilon_0 = 9.66$	

FIG. 8. Electron micrograph of MgO obtained by thermal decomposition of $MgCO_3$ (MgO-3), 600 Å grain size. Magnification 120 000×.

(1)] versus matrix refractive index are shown in Fig. 9. The separation of these curves is 1–2%, well within the uncertainty in ν_t. Moreover, ϵ_0 is probably not known to better than 1 or 2%. We believe that the results illustrated in Fig. 9 establish the nature of the strongest absorption in the MgO-1 spectrum (Fig. 1) as being of the Fröhlich type, i.e., at a frequency predicted for spheres by Eq. (1). As shown in Fig. 4, a large proportion of the particles of MgO-1 are indeed approximately spherical.

The secondary absorption in the MgO-1 spectrum is observed to shift to lower frequency with increasing refractive index of the matrix, but no detailed analysis of this shift has been made. This absorption may be due to the presence of a fairly large percentage of particles having axial ratio 2:1, apparently in the form of a pair of the approximately spherical particles stuck together. Figure 10 shows maximum-absorption frequency in MgO versus shape factor for matrix refractive indices of 1.0 and 1.5, according to Eq. (2). If these particles are assumed to approximate prolate spheroids, the shape factors for polarization parallel and perpendicular to the long axis are, respectively, $g\|=0.172$ and $g\perp=0.414$. From Fig. 10, the values of $g\|=0.172$ and $n=1.5$ yield an absorption frequency of 450 cm^{-1}, in close agreement with the experimental

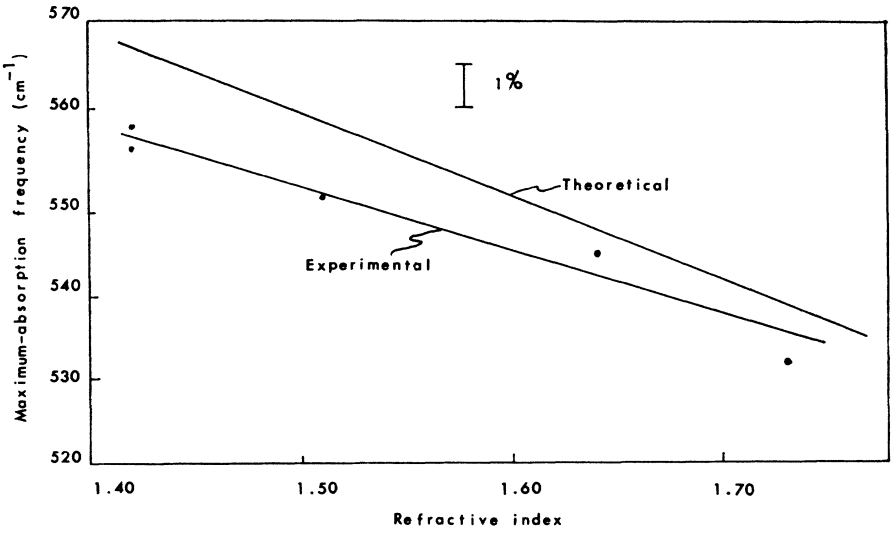

FIG. 9. Maximum-absorption frequency of commercial MgO powder (MgO-1) versus refractive index of surrounding medium.

value of 460 cm^{-1}. The absorption frequency corresponding to $g\perp = 0.414$ occurs at 540 cm^{-1}, which is too close to the spherical-particle absorption of 550 cm^{-1} to be resolved, but which would contribute, nevertheless, to the absorption in this region.

The high-frequency absorption band in the MgO-2 spectrum is interpreted in the same way as the high-frequency absorption maximum in MgO-1. This absorption, which occurs at 546 cm^{-1} for smoke deposited on polyethylene and 490 cm^{-1} for smoke in Nujol, does not result from spherical particles, which would be expected to absorb at about 605 cm^{-1} on polyethylene and at 550 cm^{-1} in Nujol. Because of the cubical shape of the smoke particles (Fig. 5), one might expect absorption at a lower frequency than in spheres. This shift is a consequence of the lower over-all depolarization effect which gives rise to smaller effective force constants than would be obtained in the case of a sphere. We have made no attempt to solve the difficult problem of computing the average depolarization (shape) factor for a cube. It may be estimated, however, from Fig. 10. From the curve for a matrix refractive index of 1.0, an absorption frequency of 546 cm^{-1} (MgO smoke on polyethylene) yields a shape factor of 0.21, which in turn predicts absorption at 500 cm^{-1} for a matrix refractive index of 1.5 (the lower curve of Fig. 10). This value is in good agreement with the 490-cm^{-1} value observed for MgO smoke in Nujol. Hence it is reasonable to conclude that the strongest absorption in the MgO-2 spectrum is of the Fröhlich type [Eq. (2)] for cubes, and that the appropriate shape factor for cubes is approximately 0.21 in place of the factor 0.33 for spheres.

The weak absorption that appears as a shoulder in the MgO-2 spectrum also may be considered as a particle-shape effect. Absorption at 665 cm^{-1} suggests

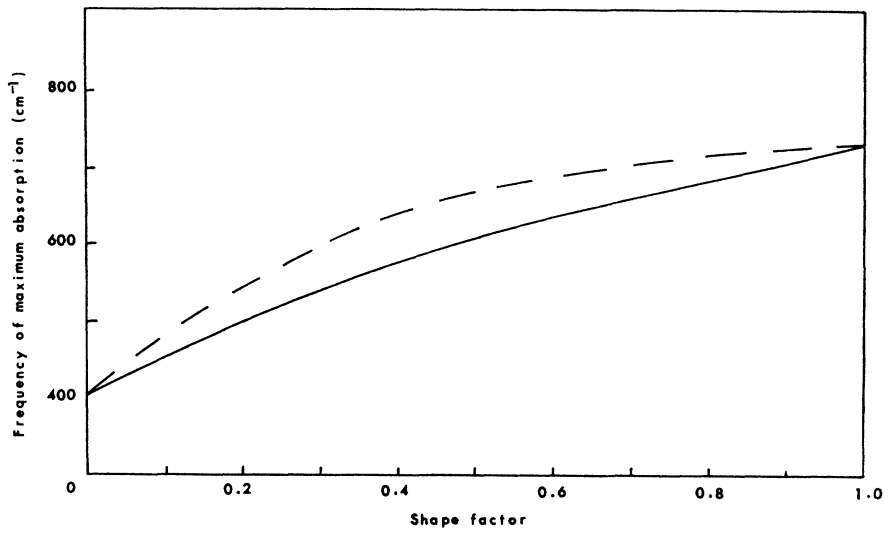

FIG. 10. Maximum-absorption frequency of MgO versus shape factor for refractive index of the surrounding medium of 1.0 (dashed line) and 1.5 (solid line).

a shape factor of approximately 0.5 for a matrix refractive index of 1.0 (Fig. 10), which factor implies an absorption frequency of 610 cm^{-1} (the lower curve of Fig. 10) for a matrix refractive index 1.5. Again this frequency agrees closely with the value of 607 cm^{-1} obtained for MgO smoke in Nujol. A shape factor of 0.5 corresponds to absorption by long, thin rodlike particles in radiation polarized perpendicular to the rod axis. Polarization parallel to such rodlike particles would cause absorption at the TO bulk-crystal frequency. Such rodlike (or chainlike) particles do occur in the MgO smoke (Fig. 5). The regularity of the stacking of the cubes in these particles suggests that they may be single crystals the growth of which has followed a characteristic pattern; we may conclude in any case that intimate contact is realized between the cubes stacked along the chain.

The primary cause for the fairly strong and sharp absorption at the TO bulk-crystal absorption frequency (401 cm^{-1}) in MgO-2 is the presence of large MgO cubes, for which the small-particle assumption is invalid. The real part of the complex refractive index of MgO rises to at least 15 at 400 cm^{-1}. This high value produces an internal wavelength of the order of $(25\,\mu)/15=1.67\,\mu$, a length comparable with the size of the larger particles. Only a few wave numbers above 401 cm^{-1}, the real part of the MgO refractive index is reduced at least by an order of magnitude, and the assumption of small particles again becomes valid. As pointed out previously, the chainlike or rodlike particles, as well as the large cubes, will absorb at the TO frequency. Neither the absorption by the long chains nor that by the large cubes will exhibit shifts with variation of the refractive index of the surrounding medium (matrix). The sharp low-frequency cutoff of this absorption is consistent with this interpretation, since the TO frequency can in no case lead to absorption below the bulk-crystal value in the harmonic approximation. Furthermore, the half-width of the peak in the real part of the complex refractive index (25–30 cm^{-1}) supports an explanation based on the presence of large particles.

The strong absorption around 400 cm^{-1} in the MgO-3 spectrum, as in the case of MgO-2, results from the presence of particles which are not small compared with the relevant radiation wavelength, that is, the internal wavelength. MgO-3 consists of large flakelike particles (many of which are several microns across) having a fine-grain structure (Figs. 6–8). Since MgO is optically isotropic, the presence of grain structures would not influence lattice-vibration absorption, i.e., a composite of small grains as a single particle would appear optically as a single crystal with the possible addition of grain-boundary perturbation. Grain boundaries produce both a broadening of the absorption and a shift to higher frequencies with decreasing grain size (cf. Fig. 3). Analysis of the grain-boundary effect has not been attempted; some conjectures, however, may be made. Both effects correlate well with the fraction of surface atoms in the grains. For a grain size of 55 Å, more than 25% of the atoms are on the surface of a grain boundary. At grain size of 380 Å, the surface atoms are fewer than 3% of the total. Up to an average grain size of 380 Å, the variation in linewidth and maximum-absorption frequency with grain size is appreciable; beyond this size there is no perceptible change in either property. The increase of linewidth with decrease in particle size probably results from inefficient irregular packing at grain boundaries. An additional effect, particularly with respect to the skewing of the absorption line towards higher frequencies for smaller grain sizes and the resultant shift in maximum-absorption frequency, may arise from the over-all shape of the particles (not to be confused with that of the grains which make up the particles). The fact that the particles of smaller grain size (Fig. 3) exhibit relatively stronger absorption at the high-frequency limit (viz., the LO bulk-crystal frequency), and at frequencies just above the TO bulk-crystal mode, as well as between, suggests the presence of particles of highly irregular shape. As discussed previously, this conjecture has been confirmed by the low-magnification electron micrograph of MgO-3 (approximately 60-Å grain size) (Fig. 6). The flakelike particles will absorb near the LO mode for polarization perpendicular to the large surface, and near the TO bulk-crystal frequency on the high side (since the particles are not infinite), for polarization parallel to this surface. Other irregularities in shape will cause absorption at intermediate frequencies. The two extreme cases cited above may be confirmed by substituting the appropriate shape factors into Eq. (2). For **E** parallel to the large surface, $g=0.0+$; for **E** perpendicular to the large surface, $g=1.0-$. For other shapes the value of g is between zero and unity.

We have observed that as average grain size increases, the grains become more clearly defined and begin to separate, i.e., strong contact is reduced (Fig. 6–8). Consequently, the *particles* will become less irregular, as sharp edges are more easily broken up in the grinding operation. This interpretation is consistent with the relatively diminishing absorption at the LO frequency and just above the TO frequency for the bulk crystal. It also accounts for the appearance of the distinct intermediate absorption for larger grain sizes. This absorption is a result of polarization-induced (Fröhlich-type) absorption in the grains themselves acting as independent particles wherever the grain boundaries between individual grains have broken down.

A second possible explanation for the absorption-frequency shift with grain size in MgO-3 is a variation in the lattice spacing. Nicholsen[11] has presented experimental evidence from low-energy electron diffraction that the lattice spacing of MgO indeed does decrease with *particle* size. We have not examined 50–1000-Å *particles* but instead *grains* inside relatively large

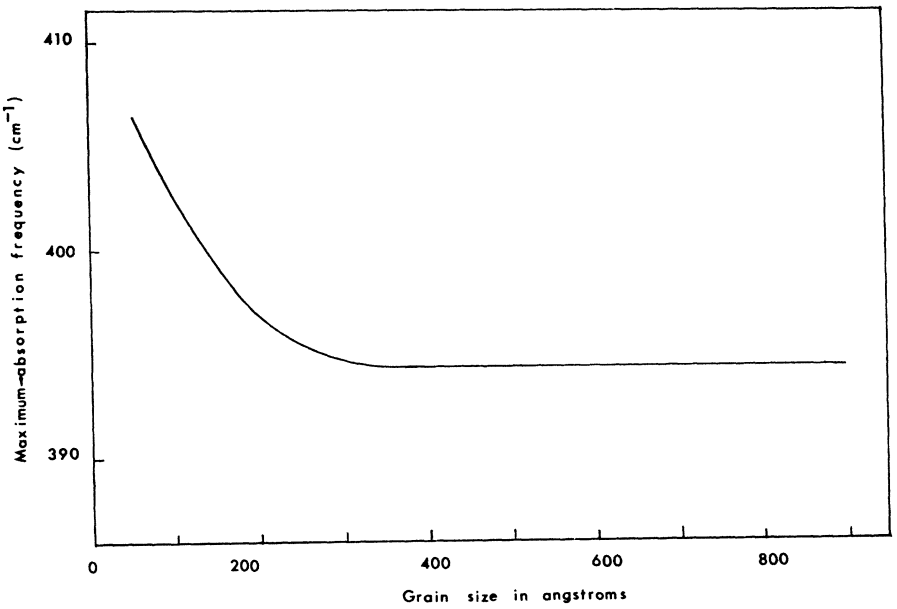

FIG. 11. Maximum-absorption frequency versus average grain size of MgO obtained by thermal decomposition of $MgCO_3$ (MgO-3).

particles. The high-energy grain boundaries may behave approximately as free surfaces, however, insofar as lattice-constant distortion is concerned. Furthermore, the grain structure would tend to inhibit the adsorption of gases, such as CO_2 or O_2, on the crystallite surfaces; such adsorption, according to Nicholsen, eliminates lattice-spacing distortion.

It is easy to establish that the magnitude of the frequency shift with grain size is consistent with the expected change in lattice spacing. Jasperse *et al.*[6] studied the infrared reflection of large MgO crystals as a function of temperature. In the temperature range 8–545 K they found a shift in the TO frequency from 408 to 394 cm^{-1}. Taking the thermal coefficient of expansion to be approximately 10^{-5} K^{-1}, we deduce a change in the MgO lattice spacing (4.2 Å) of approximately 0.02 Å. Hence, a decrease in the lattice spacing of 0.02 Å may be correlated with an increase in frequency of 14 cm^{-1}.

Anderson and Scholz[12] have found that the lattice spacing of surface atoms in ionic crystals is a few hundreths of an angstrom smaller than the lattice spacing of interior atoms in large crystals. By the use of various models and parameters they arrive at results which yield similar variations of lattice energy and lattice spacing but of somewhat different magnitudes. In any event, the decrease in lattice spacing, which is maximum at the surface, vanishes at only 30–40 atomic layers from the surface.

We have observed a frequency shift of 13 cm^{-1} (from 407 to 394 cm^{-1}) between grain sizes from 55 to about 300 Å (Fig. 11). As noted above, for a 55-Å crystallite, about 25% of the ions are surface ions; all ions, moreover, are sufficiently close to the surface to experience lattice-spacing distortion. For 380-Å crystallites, approximately 3% of the ions are on the surface; about 70% of the ions would therefore experience some lattice-spacing distortion, but to a rapidly diminishing extent as their distance from the surface increases. For 55-Å crystallites, then, maximum absorption will occur at a frequency controlled by the surface, where maximum distortion occurs, and hence at the highest frequency. On the other hand, for 380-Å crystallites the undistorted lattice will be the controlling factor in determining the frequency of maximum absorption.

Additional information on the effect of irregularities in particle shape is needed before the relative importance of these two possible mechanisms for the TO frequency shift can be established.

V. DISCUSSION

We have interpreted the infrared absorption spectra of particulate polar crystalline materials through the use of electromagnetic scattering theory and a generalized Fröhlich relation. This scheme suffices to interpret virtually all of the details of the spectra of the materials studied. Three distinct particulate forms of MgO were studied, and in all cases the spectral details were found to be consistent with theoretical computations based on size and shape of the particles.

Portions of the interpretations should not be considered as independent, particularly the interpretations of the secondary absorptions as due to double particles and long chainlike particles. The over-all success, however, of the scattering theory and Fröhlich methods in predicting the positions of the major absorptions lends credence to the interpretations of the secondary

[12] P. J. Anderson and A. Scholz, Trans. Faraday Soc. 64, 2973 (1968).

absorptions. The inability of the approach taken in this work to obtain a good fit of the theoretical transmittance curves to the experimental transmittance curves, besides predicting the frequencies of maximum absorption, is not unexpected. In all powdered materials the particles may be expected to vary in shape about some average, with some average shape factor g. Variations in shape cause line broadening which would be extremely difficult to take into account quantitatively, and the effort probably would not be justified. Size variations may result in the occurrence of absorptions of both the surface-polarization and bulk-crystal type in the same spectrum. We have semiquantitatively accounted for the effect of shape variation on linewidth by virtue of the fact that both scattering theory and the Fröhlich relation predict the presence of absorption at frequencies all the way from the bulk-crystal TO frequencies to the LO frequencies for extreme variations in particle shapes.

The success of our effort to interpret absorption spectra of particulate materials in terms of size and shape makes abundantly clear the danger of reporting absorption spectra of powdered polar materials without taking into account the effects of particle size and shape. On the other hand, with care such spectra may be interpreted and then used in support of other data. In some cases powder spectra may provide supplementary information when it is not readily available by other means. For example, when sufficiently large single crystals are not available for low-frequency reflection studies, or in the event that one or more frequencies are too low to measure with available equipment, the polarization-shifted frequency may be measurable.

PHYSICAL REVIEW VOLUME 188, NUMBER 3 15 DECEMBER 1969

Scattering-Matrix Method in Lattice Dynamics*

B. N. N. Achar† and G. R. Barsch
Materials Research Laboratory and Department of Physics, The Pennsylvania State University, University Park, Pennsylvania 16802

(Received 9 May 1969)

Localized vibrational modes of plane defects in crystals can be studied by using the scattering matrix originally introduced by Saxon and Hutner for a one-dimensional crystal model. The method is generalized and illustrated for a (001) defect plane in the rocksalt structure with general first-nearest-neighbor forces.

1. INTRODUCTION

THE scattering matrix provides a simple method for studying localized states due to impurities in crystal lattices. It was first used by Saxon and Hutner in the study of localized electronic-energy states in linear lattices[1] and applied by Fukuda to localized modes of vibration in a linear chain with isotopic defects.[2] Hori and Asahi applied the method to study the localized modes of vibration in monatomic and diatomic linear chains, with isotopic impurities at the free end.[3] They have also studied surface modes of vibration in a diatomic linear chain and a two-dimensional lattice with isotopic impurities at one edge.[3]

It is the purpose of this paper to show that the scattering-matrix method is more useful than has been generally recognized so far. It is simpler than the Green's-function method, in that the complete eigenvalue problem of the unperturbed system need not be solved beforehand. It will be shown that this method can specifically be applied to $(N-1)$-dimensional "plane" defects in N-dimensional crystal lattices; however, this domain of applicability indicates at the same time the limitation of the scattering-matrix method.

The present paper describes the generalization of the scattering-matrix method to three-dimensional crystals in the harmonic approximation. An application to the study of the localized vibrational modes in a simple cubic diatomic lattice containing a plane of isotopic impurities is made. For the special case of equal masses, this study yields the same result as obtained by Lengeler and Ludwig[4] by a different method. The correct equation for surface modes of vibration are obtained for a (100) surface of the rocksalt structure with general nearest-neighbor forces, first considered by Takeno.[5]

A subsequent paper will deal with the application of the scattering-matrix method to the study of surface modes in a semi-infinite ionic crystal.

* This work was supported by the National Science Foundation.
† Present address: Argonne National Laboratory, Argonne, Ill. 60439.
[1] D. S. Saxon and R. A. Hutner, Philips Res. Rept. 4, 81 (1949).
[2] Y. Fukuda, J. Phys. Soc. Japan 17, 766 (1962).
[3] J. Hori and T. Asahi, Progr. Theoret. Phys. (Kyoto) 31, 49 (1964).
[4] W. Ludwig, in *Theory of Crystal Defects*, edited by B. Gruber (Academic Press Inc., New York, 1966).
[5] In Ref. 2, dealing with the local vibrational modes of a one-dimensional crystal, there is an error in the definition of the S matrix. Although Fukuda uses the incorrect definition throughout his derivation, he arrives at the right condition for localized modes, namely $R_{22}=0$.

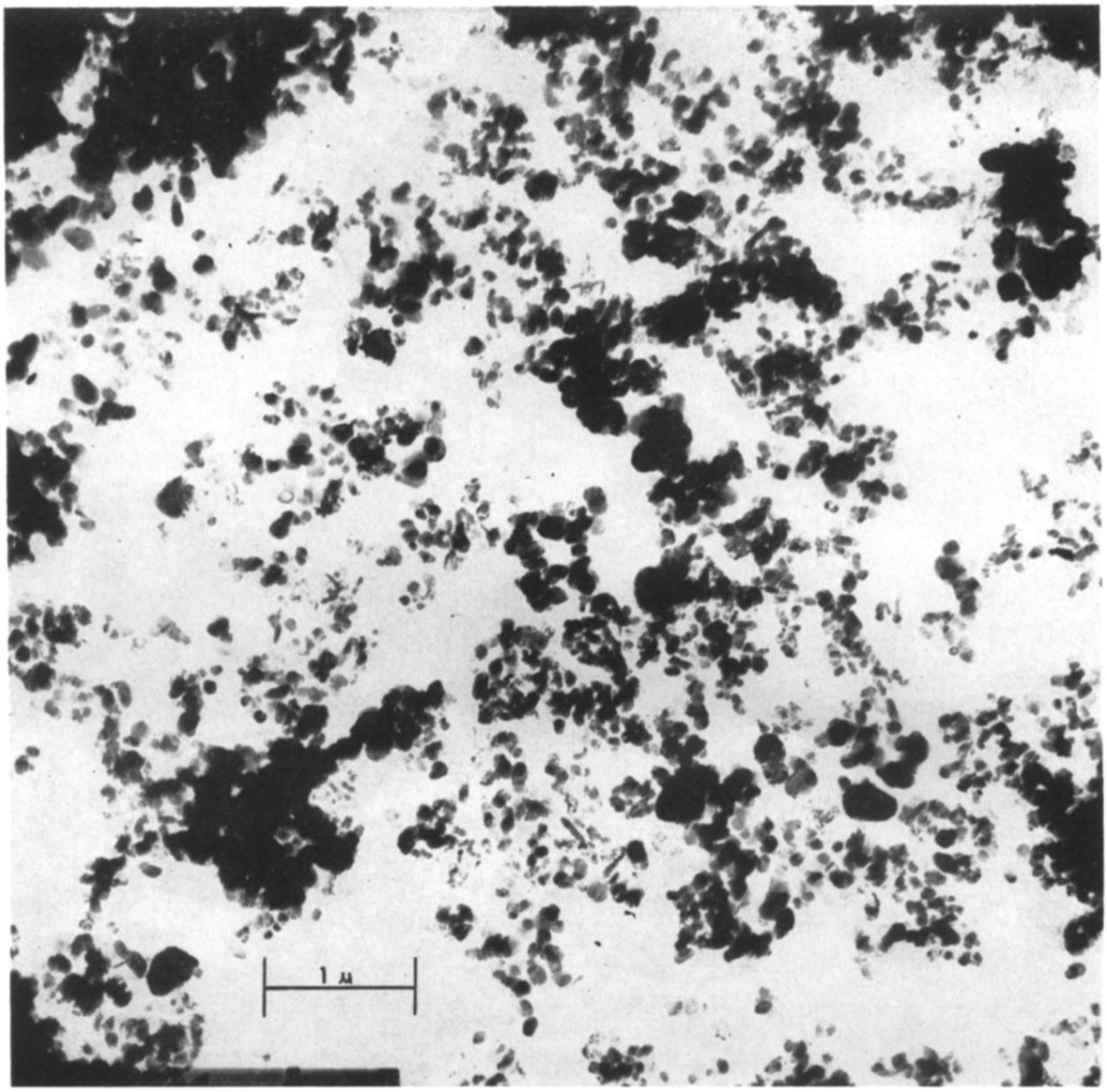

FIG. 4. Electron micrograph of commercial-grade MgO powder (MgO-1). Magnification 23 400×.

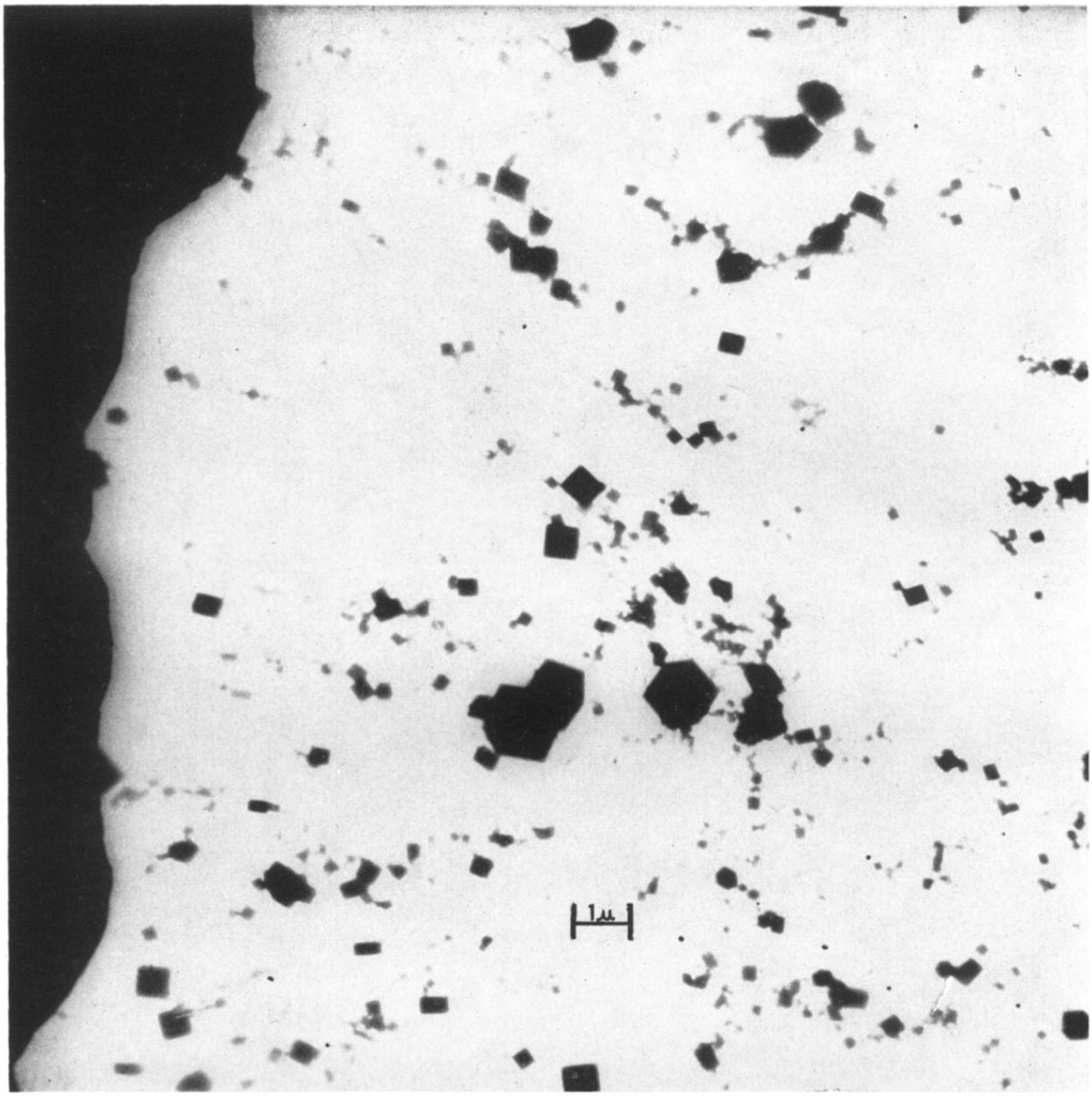

FIG. 5. Electron micrograph of MgO smoke (MgO-2) obtained by burning Mg ribbon in air. Magnification 7000×.

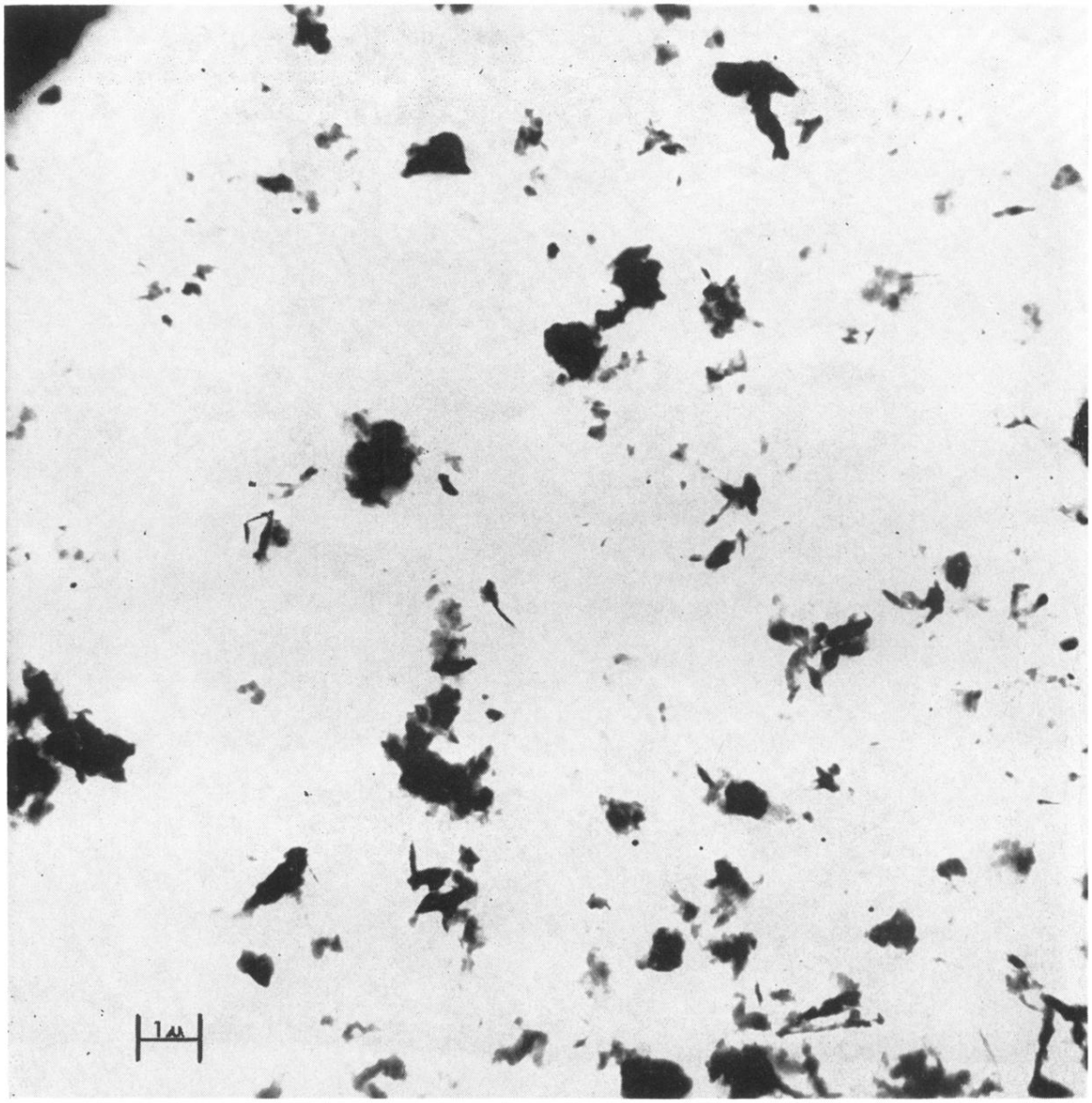

FIG. 6. Electron micrograph of MgO obtained by thermal decomposition of $MgCO_3$ (MgO-3), 60 Å grain size. Magnification 7000×.

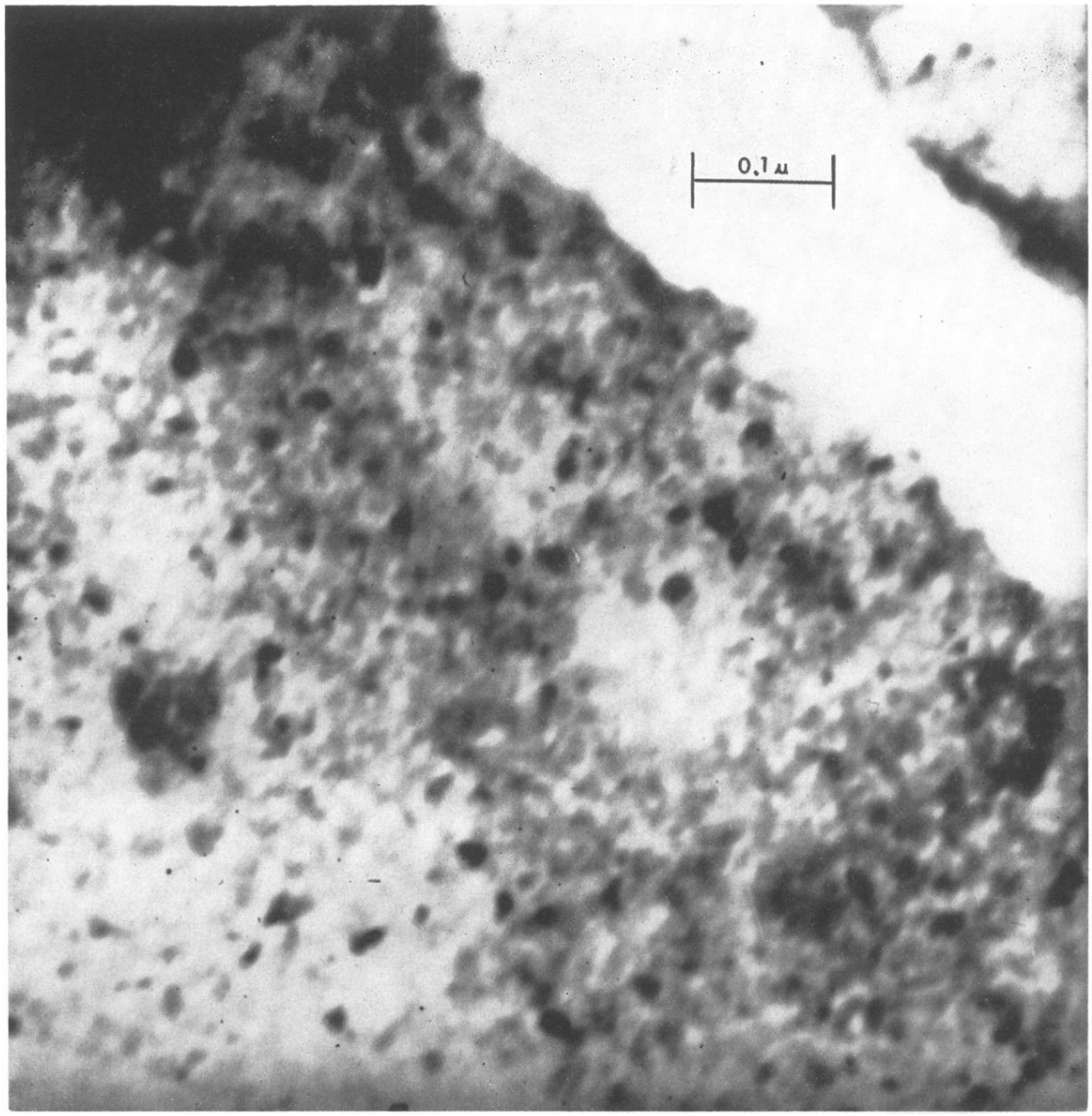

FIG. 7. Electron micrograph of MgO obtained by thermal decomposition of $MgCO_3$ (MgO-3), 100 Å grain size. Magnification 200 000×.

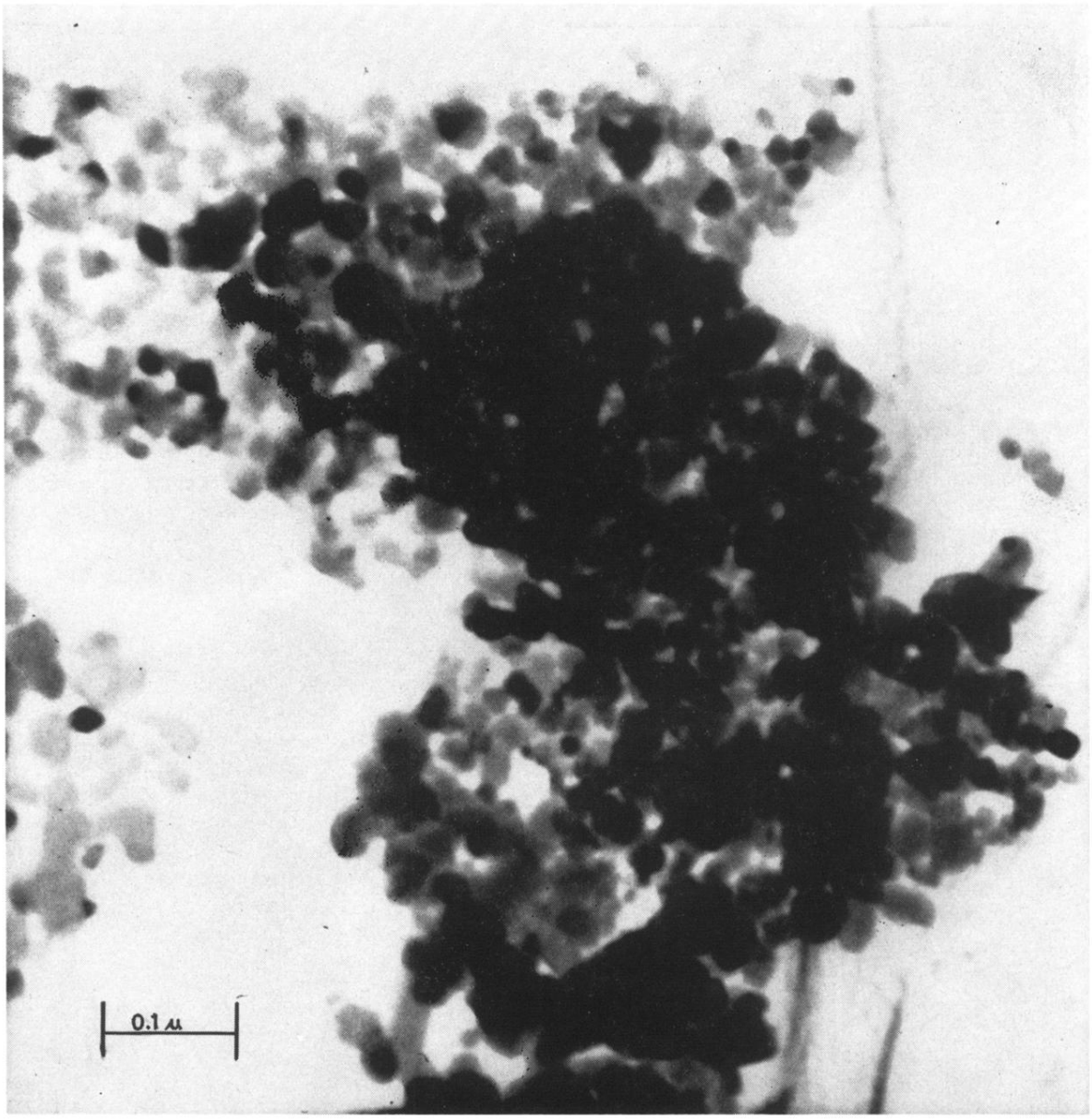

FIG. 8. Electron micrograph of MgO obtained by thermal decomposition of $MgCO_3$ (MgO-3), 600 Å grain size. Magnification 120 000×.